Bulletin of the National Research Centre

RESEARCH Open Access

Statistical optimization of chemical modification of chitosan-magnetic nano-particles beads to promote *Bacillus subtilis* MK1 α-amylase immobilization and its application

Mohamed A. A. Abdella[1], Gamal M. El-Sherbiny[2], Aliaa R. El-Shamy[1], Sherien M. M. Atalla[1] and Samia A. Ahmed[1*]

Abstract

Background: α-Amylase randomly hydrolyzes starch molecule to produce oligosaccharides of different chain length. It is among the most significant hydrolytic enzymes used in industrial applications. Enzyme immobilization is the simplest way to solve the stability problem of protein under industrial harsh conditions. Magnetic nano-particles considered suitable for immobilization due to their unique characteristics. The polymer nanocarriers still the feature of modifiable surfaces of carriers for further conjugation with biomolecule. This study aims to promote the immobilization of *Bacillus subtilis* MK1 α-amylase using the statistical optimization of the chemical modification of the chitosan-magnetic nano-magnetic particle beads and their ability to apply.

Results: *B. subtilis* MK1 α-amylase was successfully immobilized on chitosan-magnetic nano-particles using a method combining the advantages of both physical adsorption and covalent binding. The beads were chemically modified using polyethyleneimine (PEI) followed by glutaraldehyde (GA). Aminated beads by (PEI), activated beads by (GA), and immobilized enzyme on activated beads were characterized using FTIR. Morphological examinations of the beads surface before and after conjugation with the α-amylase enzyme were carried out using scanning electron microscope (SEM). Chemical modification parameters of the beads were optimized using response surface methodology based on central composite design. Statistical approach enhanced the immobilization yield (IY%) by 1.5-fold. The application of immobilized enzyme in the baking process enhanced dough-raising about 2.3-fold and can be reused for 5 cycles with 100% activity.

Conclusions: Statistical methods are an important way to improve immobilization yield and efficiency. The ANOVA data confirmed the fitness of the model which possessed R^2 value (0.975) and the adjusted R^2 value (0.940). The results confirm the ability to reuse the immobilized enzyme in industrial processes.

Keywords: α-Amylase, Chitosan-magnetic nano-particles, Beads modification, Cross-linker, Central Composite design

* Correspondence: dr_sa_ahmed@yahoo.com
[1]Chemistry of Natural and Microbial Products Department, National Research Centre, Dokki, Cairo, Egypt
Full list of author information is available at the end of the article

Introduction

Enzymes have numerous characteristics, and they are more preferable over chemical catalysts in many areas of industry ranging from food to pharmaceuticals (Zdarta et al. 2018). α-Amylase (*EC* 3.2.1.1) randomly hydrolyzes α-1,4-glycosidic bonds in the interior of starch molecule (Fig. 1) to produce branched and linear oligosaccharides of different chain length (Simair et al. 2017; Frantz et al. 2019). Amylases are among the most significant hydrolytic enzymes that are used in various industrial applications including food production (fruit juice clarification, bread, baking, and beer industries), textiles, detergents, pharmaceutical, pulp and paper, ethanol, and biofuel production (Yang et al. 2014; Tambekar et al. 2016; Pandey et al. 2017; Frantz et al. 2019).

High stability of enzyme under industrial conditions is considered an economic advantage due to low enzyme loss. Enzyme immobilization is the simplest way to solve the stability problem of protein and reduce the expensive cost of applying them on an industrial scale (Ahmed et al. 2019a, 2019b). Also, immobilization improves enzyme properties as activity, reduces the inhibition, increases stability, specificity to substrates, and avoids contamination of product by enzyme (Ahmed et al. 2019a, 2019b).

Immobilization of enzymes can offer many benefits as reusability and recovery from their products enhance stability under both operational and storage conditions (Souza et al. 2019). Enzymes immobilization on nano-carriers results in stabilization of active conformation, which enhances the interfacial reactions between the enzyme active sites and its substrate. The nano-environment surrounding enzyme molecules prevent enzyme deactivation (Misson et al. 2015). Nano-particles have high adsorption capacities, large specific surface areas, high mobility in porous media because of their specific functionality, surface area per unit mass, and smaller size than the relevant pore spaces and the ease of modifying their surface functionality (Swelam et al. 2019). Also, magnetic nano-particles as Fe_3O_4, γ-Fe_2O_3, ZnO, and TiO_2 are considered significant carriers that enhance immobilization efficiency because they have high stability and high electron conductivity.

Fe_3O_4 nano-particles are considered suitable for immobilization due to their unique characteristics (small size, super-paramagnetism, tailored surface chemistry, low toxicity, biocompatibility, and biodegradability). The magnetic Fe_3O_4 nano-materials are generally unstable under acidic solutions and undergo leaching which leads to reduction of its lifetime (Sojitra et al. 2017).

Furthermore, magnetic nano-particles coated with organic/inorganic molecules as polymers are more effective for the free functional groups present on the surface due to providing a large number of active sites (Swelam et al. 2019). The polymer nano-carriers still the feature of modifiable surfaces of carriers for further conjugation with biomolecule (Misson et al. 2015).

Chitosan is a natural polymer known as an ideal carrier for enzyme immobilization. It is cheap, non-toxic, and has good (hydrophilicity, biocompatibility and adhesion) and high affinity towards proteins (Bindu et al. 2018). In addition, amino groups of chitosan are useful for conjugation with enzyme protein via cross-linking agents such as glutaldehyde (Kuo et al. 2012).

Enzyme immobilization includes different methods such as physical adsorption, entrapment, covalent binding, and cross-linking to solid carrier. Physical adsorption is the simplest immobilization method showing low stability after repeated use due to the weak bonds between enzyme and carrier surface as van der Waals and hydrogen bonding.

However, the immobilization by covalent binding is considered the most effective method because of increasing the enzyme stabilities. Also, covalent immobilization may be an encouraging procedure in establishing enzymes

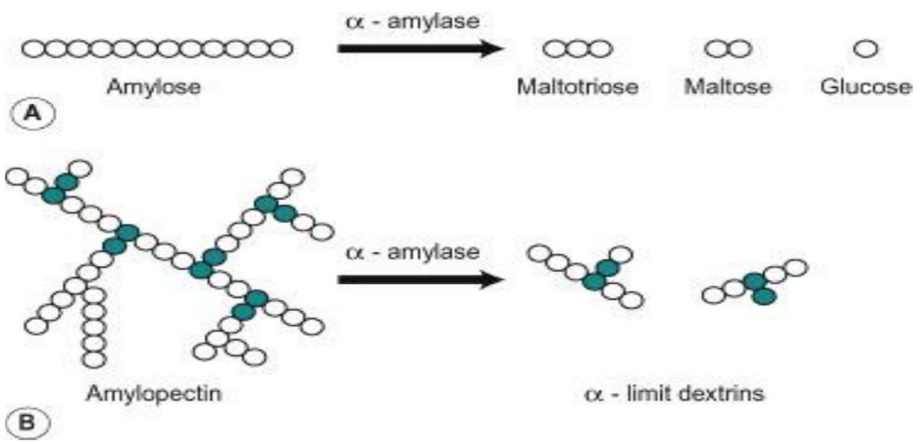

Fig. 1 Schematic representation of starch (amylose and amylopectin) and mode of action of α-amylase

and inhibiting their leakage because of the formation of covalent bonds between enzyme and carrier surface (Eskandarloo and Abbaspourrad 2018). A method was developed that combines the advantages of both physical adsorption and covalent bonding methods (Wang et al. 2015). The immobilization yield (IY%) is the key parameter since it represents the general output of the efficiency of the immobilization process (Ahmed et al. 2008).

Response surface methodology (RSM) is a statistical and mathematical mechanism used for constructing models, designing experiments, and examining the optimum conditions affecting the IY%. It was performed through combination of some independent variables involved in the experimental design for promoting the IY of enzyme. Furthermore, RSM based on central composite design (CCD) reduces the number of individual experiments desired for providing information on the interactions between different variables to define the most significant factors (Abdel Wahab and Ahmed 2018).

In the current study, α-amylase enzyme was immobilized onto chitosan-magnetic nano-particles (Ch-MNP) beads using physical adsorption and covalent binding in order to increase its activity and stability. Ch-MNP beads modification to promote IY% was optimized using statistical methods. Finally, the chitosan-magnetic nano-particles/polyethyleneimine/glutaraldehyde/enzyme (Ch-MNP/PEI/GA/Enz) was applied in the baking industry.

Materials and methods

Materials

Chitosan (Mw 50–90 kDa with DD of 80%) was supplied from Sigma Chemical, Co., St. Louis, USA.

Polyethyleneimine (PEI, 50%, w/v), glutaraldehyde (GA, 50%, w/v), 3,5-dinitrosalicylic acid (DNS98%), and sodium hydroxide 97% (Mw 40 g/mol) were obtained from Sigma-Aldrich, Chemie GmbH, Riedstr. 2, D-89555 Steinheim, Germany. Soluble starch 99% (Mw 342.3 g/mol) and potassium sodium tartrate (Rochelle salt, 99%, Mw 282.23 g/mol) were obtained from WINLAB, UK. Other chemicals were of analytical grade.

Methods

Enzyme production

α-Amylase enzyme was produced under submerged fermentation from isolated strain *B. subtilis* strain-MK1 as reported in the previous work by Ahmed et al. 2019a, 2019b. The enzyme was partially purified using 60% (v/v) ethanol precipitation; the precipitate was collected by centrifugation, dried, weighed, and used for α-amylase immobilization.

Preparation of chitosan-magnetic nano-particles (Ch-MNP) beads

Magnetic nano-particles (Fe_3O_4) were prepared according to Mehta et al. (2006) with some modifications. The method depended on mixing ferric and ferrous ions in a 1:2 molar ratio in highly basic solution at elevated temperature. In brief, iron (III) chloride hexahydrate (0.0551 mol) was dissolved in 150 mL of ammoniated water while 0.0275 mol of iron (II) chloride tetrahydrate was dissolved in 150 mL of ammoniated water. Then, the two solutions were mixed in a 500 mL conical flask and placed in a temperature-controlled water bath equipped with a magnetic stirrer. A sodium hydroxide aqueous solution (12.8 g in 120 mL of distilled water) was then added with a flow rate of 10 mL/min while continuously stirring at 80 °C, and the reaction was continued for 60 min under the same conditions. The resulting Fe_3O_4 particles were washed 3 times repeatedly with 500 mL of distilled water until neutral pH using magnetic field separation and finally kept in 150 mL distilled water in the fridge for further treatment.

Chitosan was dissolved in distilled water to produce 2% (w/v) solution then mixed with a solution of magnetic nano-particles (Fe_3O_4). After that, the polymer solution was sprayed into cross-linking solution of NaOH 5% (w/v), through a nozzle of 300 μm using the Inotech Encapsulator. The prepared beads were hardened in cross-linking solutions for 3 h. To modify the gel beads for covalent immobilization of enzyme, the gel beads were soaked in a solution of 4% (v/v) polyethylenimine (PEI) at pH 9.5 for 3 h, followed by soaking in glutaraldehyde (GA) 2.5% for 3 h, and after washing, the gel beads was ready for immobilization (Yuan et al. 2016).

Enzyme binding to activated beads

Partially purified α-amylase from *B. subtilis* strain-MK1 was immobilized by covalent binding on Ch-MNP. This was performed by mixing 2 mL of the partially purified α-amylase (200 U) with 1 g of the activated beads. The mixture was left for 24 h at 4 °C, and then the beads were washed twice with distilled H_2O and were used for enzyme assay (Abdel Wahab et al. 2018).

Determination of α-amylase activity

α-Amylase activity was done according to Sajjad and Choudhry (2012) by mixing 0.5 ml of 1% soluble starch in 0.1 M phosphate buffer (pH 7.0) with 0.5 mL of the partially purified enzyme or 0.2 g of immobilized enzyme and was incubated for 30 min at 40 °C. The reaction was stopped by adding 1 mL of dinitrosalicylic acid (DNS) reagent and kept on boiling water bath for 10 min (Miller 1959), and the color absorbance was read at 540 nm. One unit of enzyme activity (U) is defined as the

Fig. 2 α-Amylase immobilization on Ch-MNP/PEI/GA beads

amount of enzyme that liberated 1 μmol of reducing sugar as glucose/min under assay conditions. All the experiments were performed in triplicate, and the results were expressed as mean values. Immobilization yield (IY%) was calculated according to Wang et al. (2015) as following:

$$\text{IY}\ (\%) = I/(A–B) \times 100$$

where I is the total activity of immobilized enzyme, *A* is the total activity offered for immobilization, and *B* is the total activity of unbounded enzyme.

Optimization of beads modifications using statistical design

Response surface methodology (RSM) based on central composite design (CCD) was used to determine the optimum level of four important factors for beads modification of Ch-MNP beads. These factors include PEI percent (%) (W), PEI activation time (X), GA percent (%) (Y), and GA activation time (Z). These factors were tested at three levels as, low (− 1), central (0), and high (+ 1), resulting in experimental design of 25 experiments with respect to mean of IY (%) of α-amylase on Ch-MNP beads as response. The experimental data were analyzed by the response surface regression procedure to fit the second order polynomial of the equation:

$$\text{IY} = \beta_0 + \Sigma\beta_i X_i + \Sigma\beta_{ii} X_i^2 + \Sigma\beta_{ij} X_i X_j$$

where IY represents response, β_0 is the interception coefficient, β_i is the coefficient of the linear effect, β_{ii} is the coefficient of quadratic effect, β_{ij} is the coefficient of the interaction effect, and X_iX_j are the independent variables which influence the response variable (IY). All the experiments were performed in triplicate, and the results were expressed as mean values. The independent variables of the experimental design were optimized and interpreted using the (JMP) statistical software.

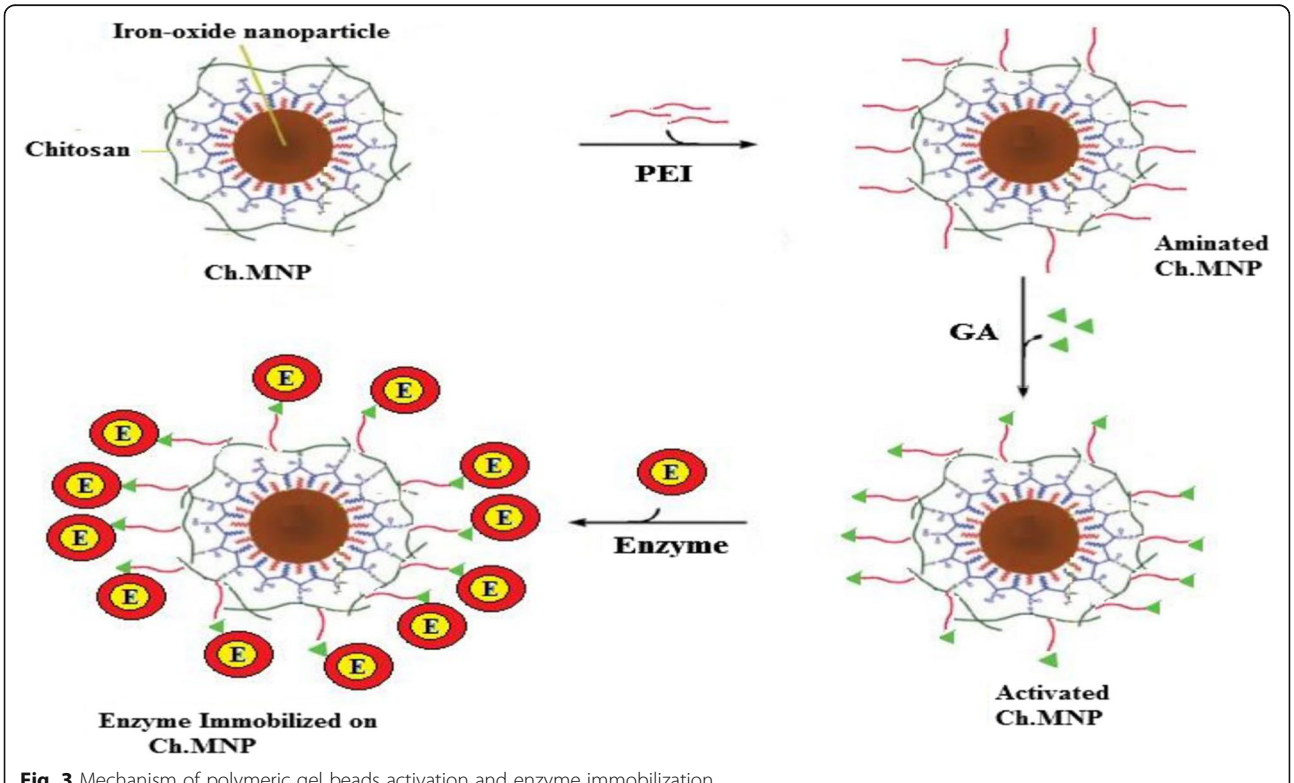

Fig. 3 Mechanism of polymeric gel beads activation and enzyme immobilization

Statistical analysis of data

Statistical analysis of the model was carried out according to the analysis of variance (ANOVA). The quality of the fit of the polynomial model equation was assessed by determining the R^2 coefficient and the adjusted R^2 coefficient. Also, the significance of statistical and regression coefficient were checked with F test and P value, respectively. The validation of the model was checked by the comparison of experimentally obtained data with the predicted values, and the prediction error was calculated. Three-dimensional (3D) surface plots and corresponding contour plots were constructed to explain the effect of the independent variables on the responses (IY).

Fourier transforms infrared (FTIR) spectroscopy analysis

The FTIR absorption spectra of Ch-MNP/PEI/GA (beads), free α-amylase enzyme, and Ch-MNP/PEI/GA/Enz (immobilized enzyme) were measured by FTIR spectroscopy attenuated total reflection (ATR) mode Bruker VERTEX 70/70v model using the KBr disk technique. This test was performed to detect the presence of the new functional group and carbonyl group formed at all different formulas. The reaction began by mixing 2% (w/w) of the sample with dry KBr. The mixture was ground into a fine powder using an agate mortar before it was compressed into a KBr disk under a hydraulic press at 10,000 psi. Each KBr disk was scanned over a wave number range of 400–4000 cm^{-1}, with a resolution of 4 cm^{-1}, and the characteristic peaks were recorded.

Scanning electron microscope (SEM)

These investigations were performed in order to describe the morphological changes on the beads surface before and after conjugation with the enzyme. Morphological examinations on the surface of Ch-MNP and Ch-MNP/PEI/GA/Enz were carried out using scanning electron microscopy (SEM, Quanta 250 FEG, accelerating voltage 200 V–30 kV, FEI Company, Thermo Fisher Scientific).

Application of Ch-MNP/PEI/GA/enzyme in baking process

For studying application of immobilized α-amylase in baking process, dough was prepared by using 50 g wheat flour, 1.0 g baker's yeast, 1.0 g Ch-MNP/PEI/GA/Enz (200 U), and 5 mL of H_2O (Ahmed et al. 2016). Dough-raising was observed carefully after incubation at room temperature (~ 35 °C) for 2 h and was compared with control (dough without enzyme). After each run, the beads were washed with sodium phosphate buffer (0.1 M, pH 8.0) to remove any residual substrate and reused to start a new run.

Results

Enzyme immobilization

Ch-MNP beads were chemically modified using PEI followed by GA. *B. subtilis* MK1 α-amylase was successfully immobilized on activated Ch-MNP beads with high immobilization yield 55% (Fig. 2). The activated beads reacted with the enzyme molecule as shown in Fig. 3. The reaction happened between the NH_2 group found in the enzyme protein molecule, and the free C=O group located on GA forming C=N–bond.

Central composite statistical design (CCD) for optimization of beads modifications

The CCD of the coded variables and the corresponding experimental results of the IY% are displayed in Table 1. By using a multi-regression analysis for the experimental results, the predicted IY (%) of α-amylase was acquired from the following second-order polynomial equation:

Table 1 CCD experimental and predicted values of Ch-MNP/PEI/GA/α-amylase immobilization yield

Run	W: PEI [%]	X: PEI activation time [h]	Y: GA [%]	Z: GA activation time [h]	Immobilization yield [%]	
					Actual	Predicted
1	0 (4)	0 (3)	0 (2.5)	+ 1 (4)	64.2	63.2
2	+ 1 (6)	− 1 (2)	− 1 (1)	+ 1 (4)	52.2	53.4
3	− 1 (2)	0 (3)	0 (2.5)	0 (3)	58	58.1
4	0 (4)	0 (3)	0 (2.5)	0 (3)	57	57.4
5	− 1 (2)	− 1 (2)	+ 1 (4)	+ 1 (4)	57.7	58.1
6	0 (4)	+ 1 (4)	0 (2.5)	0 (3)	51.8	53.4
7	− 1 (2)	+ 1 (4)	− 1 (1)	+ 1 (4)	61.2	63
8	+ 1 (6)	+ 1 (4)	− 1 (1)	+ 1 (4)	59.1	57.9
9	0 (4)	0 (3)	+ 1 (4)	0 (3)	62.2	64.5
10	− 1 (2)	− 1 (2)	− 1 (1)	+ 1 (4)	56.5	56.4
11	0 (4)	− 1 (2)	0 (2.5)	0 (3)	48.2	46.5
12	+ 1 (6)	− 1 (2)	+ 1 (4)	− 1 (2)	73.8	73.3
13	− 1 (2)	− 1 (2)	− 1 (1)	− 1 (2)	51.6	52.2
14	+ 1 (6)	+ 1 (4)	− 1 (1)	− 1 (2)	62.1	63
15	+ 1 (6)	− 1 (2)	− 1 (1)	− 1 (2)	54.9	55.3
16	− 1 (2)	+ 1 (4)	+ 1 (4)	− 1 (2)	70.5	70.6
17	− 1 (2)	− 1 (2)	+ 1 (4)	− 1 (2)	61.2	61.2
18	0 (4)	0 (3)	− 1 (1)	0 (3)	57.4	54.9
19	+ 1(6)	0 (3)	0 (2.5)	0 (3)	61.8	61.6
20	0 (4)	0 (3)	0 (2.5)	− 1 (2)	66.4	67.3
21	+ 1 (6)	+ 1 (4)	+ 1 (4)	+ 1 (4)	67.3	68
22	+ 1 (6)	− 1 (2)	+ 1 (4)	+ 1 (4)	64.3	64.1
23	+ 1 (6)	+ 1 (4)	+ 1 (4)	− 1 (2)	81.6	80.5
24	− 1 (2)	+ 1 (4)	− 1 (1)	− 1 (2)	63.2	62.1
25	− 1 (2)	+ 1 (4)	+ 1 (4)	+ 1 (4)	65.9	64.2

$$\begin{aligned} IY(\%) = {} & 57.3542 + 1.7388\,W + 3.4611X \\ & + 4.7944Y - 2.05Z - 0.5562WX \\ & + 2.2437WY - 1.5187WZ - 0.1312XY \\ & - 0.8187XZ - 1.8187YZ + 2.4867W^2 \\ & - 7.4132X^2 + 2.3867Y^2 + 7.8867Z^2 \end{aligned}$$

where I is the predicted IY (%); W, X, Y, and Z are the code values of PEI percent (%), PEI activation time, GA percent (%), and GA activation time, respectively.

The highest IY of α-amylase (81.6%) was obtained in trail no.23 under optimizing conditions of 6% PEI, 4 h PEI activation time, 4% GA, and 2 h GA activation time as shown in Table 1. The ANOVA data is displayed in Table 2 and confirmed the great significance of the model which possessed F value of 27.914, low P value of < 0.0001. According to the results, the value of R^2 was 0.975, and the adjusted R^2 was 0.940 which is close to R^2 value. The estimation coefficients, standard errors, t test values, and P values are illustrated in Table 3, and the data displayed the significance of linear, interaction, and quadratic terms. As shown in Fig. 4, the Pareto chart interpreted that GA (%) possessed the most significant influence flowed by PEI activation time and PEI (%) that affected IY of α-amylase positively, whereas GA activation time exhibited negatively significant effect. The closing between the actual values and predicted values of IY indicated the good precision and validation of the model (Fig. 5). The normality assumption was satisfied as the residual plot approximated along a straight line as given in Fig. 6. The results reported in Fig. 7a–f of the 3D surface interactions investigated that figures of interaction terms (WY, WZ, and YZ) showed significant effect, while figures of interaction terms (WX, XY and XZ) showed insignificant effect on IY of α-amylase. Finally, optimization of beads modifications enhanced the IY by 1.5-fold compared with un-optimized.

Scanning electron microscope (SEM) characterization

Scanning electron microscopy showed the modification which occurred during gel beads formation, activation, and immobilization. A remarkable change in pore size before and after immobilization is displayed in Fig. 8a–b. Noticeable changes were recognized along the steps of gel beads formation and accumulation of enzyme on the gel beads surface after immobilization.

FTIR characterization

FTIR spectroscopic analysis of activated beads (Ch-MNP/PEI/GA) (A), immobilized α-amylase on activated beads (Ch-MNP/PEI/GA/Enz) (B), and free α-amylase enzyme (C) were carried out in a range varied from 400–4000 cm^{-1}. As seen in Fig. 9, the typical characteristic absorption bands of modified activated chitosan beads and free α-amylase enzyme in accordance with the literature appeared. Activated beads showed two peaks, one of them at 1730 cm^{-1} corresponding to the (C=O) group of GA free end, and the second one is at 1650 cm^{-1} corresponding to the (C=N–) group that was

Table 2 Analysis of variance (ANOVA) for CCD

Source	Sum of squares	Df	Mean square	*F* value	*P* value Prob > F	
Model	1290.78	14	92.1986	27.914	< 0.0001*	Significant
W: PEI %	54.4272	1	54.4272	16.4782	0.0023*	Significant
X: PEI activation time	215.6272	1	215.6272	65.2825	< 0.0001*	Significant
Y: GA %	413.7606	1	413.7606	125.2686	< 0.0001*	Significant
Z: GA activation Time	75.645	1	75.6450	22.9020	0.0007*	Significant
WX	4.9506	1	4.9506	1.4988	0.2489	
WY	80.5506	1	80.5506	24.3872	0.0006*	Significant
WZ	36.9056	1	36.9056	11.1734	0.0075*	Significant
XY	0.2756	1	0.2756	0.0834	0.7786	
XZ	10.7256	1	10.7256	3.2473	0.1017	
YZ	52.9256	1	52.9256	16.0236	0.0025*	Significant
W^2	15.7487	1	15.7487	4.7680	0.0539	
X^2	139.9616	1	139.9616	42.3743	< 0.0001*	Significant
Y^2	14.5075	1	14.5075	4.3922	0.0625	
Z^2	158.4097	1	158.4097	47.9595	< 0.0001*	Significant
Error	33.0299	10	3.3030			
C. Total	1323.8096	24				

R^2 = 0.975, Adj R^2 = 0.940, significant ($P \leq 0.05$), non-significant ($P > 0.05$)
Df degree of freedom

Table 3 Statistical analysis of CCD showing coefficients, *t*- values, *P*-values and standard errors

Term	Coefficient estimate	Std Error	*t* ratio	*P* value Prob > F	VIF
Intercept	57.3542	0.78473	73.09	< 0.0001*	1
W: PEI %	1.7389	0.42836	4.06	0.0023*	1
X: PEI activation time	3.4611	0.42836	8.08	< 0.0001*	1
Y: GA %	4.7944	0.42836	11.19	< 0.0001*	1
Z: GA activation time	− 2.05	0.42836	− 4.79	0.0007*	1
WX	− 0.5562	0.45435	− 1.22	0.2489	1
WY	2.2437	0.45435	4.94	0.0006*	1
WZ	− 1.5187	0.45435	− 3.34	0.0075*	1
XY	− 0.1312	0.45435	− 0.29	0.7786	1
XZ	− 0.8187	0.45435	− 1.80	0.1017	1
YZ	− 1.8188	0.45435	− 4.00	0.0025*	1
W^2	2.4867	1.13883	2.18	0.0539	1.9789
X^2	− 7.4132	1.13883	− 6.51	< 0.0001*	1.9789
Y^2	2.3867	1.13883	2.10	0.0625	1.9789
Z^2	7.8867	1.13883	6.93	< 0.0001*	1.9789

produced from the reaction with GA (curve A). While immobilized enzyme on beads give broader peak at 3457 cm^{-1}, pointed to increasing NH_2 group's concentration (curve B). When comparing with free α-amylase enzyme (curve C), we can notice that the characteristic peaks of enzyme, at 3434 cm^{-1} and at 1117 cm^{-1}, are found in curve (B).

Application of Ch-MNP/PEI/GA/Enz in baking process

As shown in Fig. 10, treated dough with 1 g beads of Ch-MNP/PEI/GA/Enz enhanced dough-raising about 2.3-fold as compared to the control (without enzyme). Ch-MNP/PEI/GA/Enz could be easily separated from the dough and reused for 5 consecutive cycles with 100% residual activity.

Discussion

Immobilized enzyme is required for the development of industrial applications in order to minimize the cost of the biocatalyst. As shown in Fig. 2, α-amylase from *B. subtilis* MK1 was immobilized on Ch-MNP/PEI/GA beads and exhibited 55% IY. Ahmed et al. (2018) reported that α-amylase was immobilized on phosphosilicate glass with lower IY (27.9%). The activated beads reacted with the enzyme molecule as shown in Fig. 3. The reaction happened between the NH_2 group found in the enzyme protein molecule and the free C=O group located on GA (the cross-linker) forming C=N– bond as reported by Yuan et al. (2016). Magnetic nano-particles have unique properties as high affinity to proteins and ability to be chemically modified with reactive functional groups (Atacan et al. 2016). Misson et al. (2015)

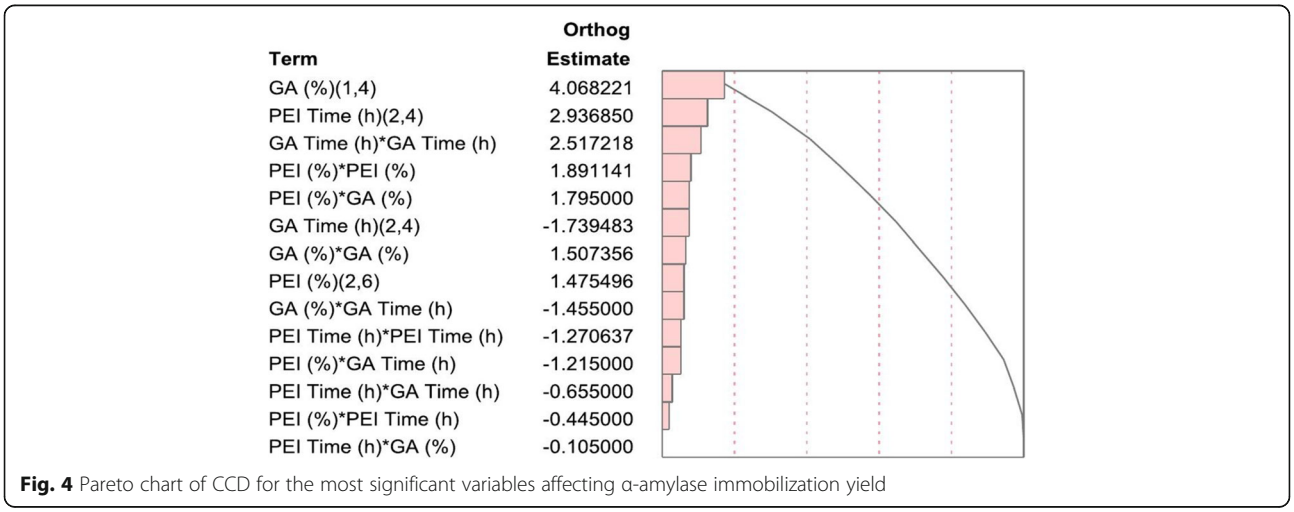

Fig. 4 Pareto chart of CCD for the most significant variables affecting α-amylase immobilization yield

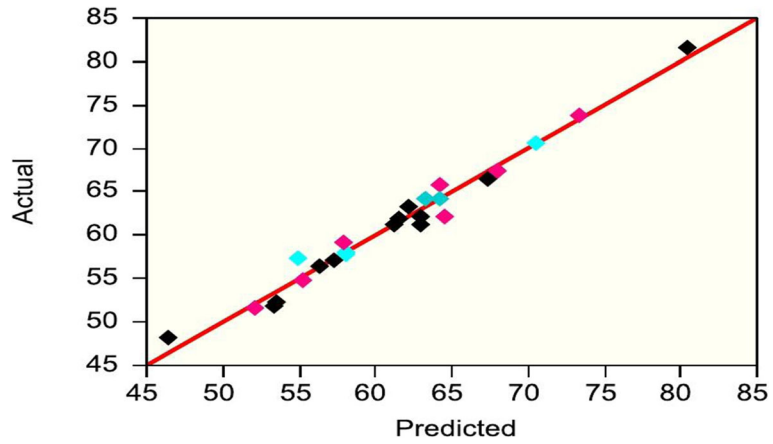

Fig. 5 CCD for the relation between actual and predicted α-amylase immobilization yield

reported that, polymeric nano-carrier can be fabricated easily in nanometer scale with a large surface area in the range of 30–500 nm.

Statistical optimization of carrier modification by CCD of the coded variables and the corresponding experimental results of the IY% are displayed in Table 1. It was found that, trail no.23 gives the highest IY of α-amylase (81.6%) at optimizing conditions of 6% PEI, 4 h PEI activation time, 4% GA, and 2 h GA activation time. Lower result was obtained by Ahmed et al. (2018) after statistical optimization of the immobilization conditions (79.9% IY). Hassan et al. (2019) found that lower concentration of PEI (1%) and GA (0.5) was suitable to activate κ-carrageenan gel beads.

The analysis of variance (ANOVA) was performed to examine the effectiveness of the quadratic model equation for the immobilization as presented in Table 2. The low probability value (Prob > F or P value ≤ 0.05) and F value proved that the model is potent and highly significant. The ANOVA data confirmed the great significance of the model which possessed F value of 27.914 and low P value of < 0.0001, and there is only 0.01 % chance that this value might occur due to noise. Furthermore, the determination coefficient (R^2) evaluated the fineness of the model where the R^2 value becomes nearer to 1.0. According to the results, the R^2 value was 0.975 indicating that 97.5 % of the response variability could be analyzed by the statistical model. A regression model, with R^2 (0.975) was considered to have very high correlation (Jaya et al. 2010). Also, the adjusted R^2 value was 0.940 and closer to R^2 value which demonstrated the suitability of this model. On the other hand, the estimation coefficients, standard errors, t test values, and P values are illustrated in Table 3, and the data displayed the significance of linear, interaction, and quadratic terms. The data indicated that, linear terms (W, X, Y, Z), interaction terms (WY, WZ, YZ), and quadratic terms (X^2, Z^2) were significant ($P \leq 0.05$), while

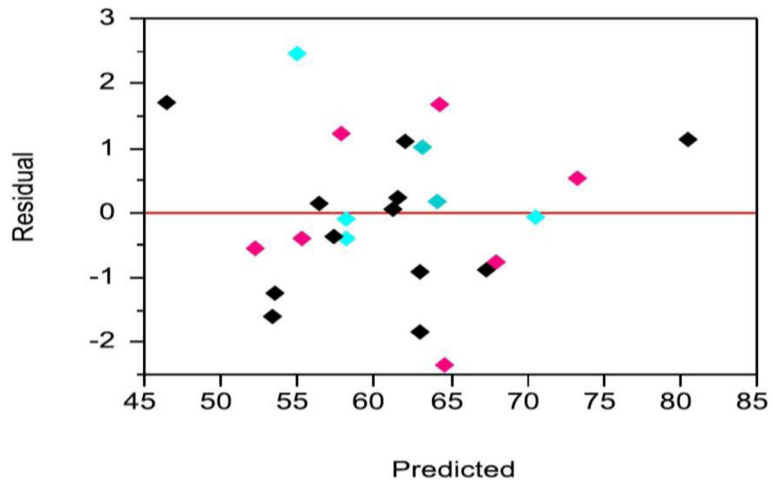

Fig. 6 The relation between predicted and residual values of α-amylase immobilization yield

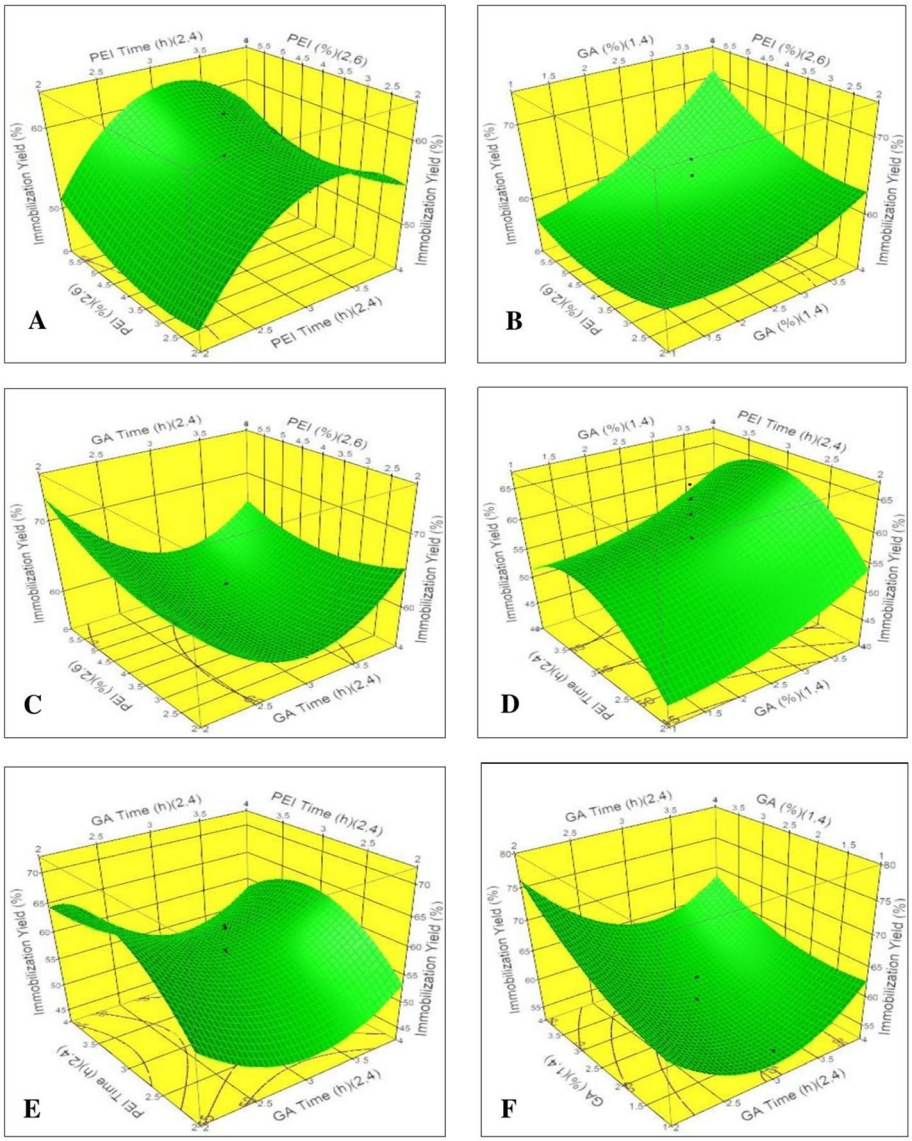

Fig. 7 The 3D surface plots representing interaction between factors affecting IY of α-amylase. **a** PEI percent and PEI activation time. **b** PEI percent and GA percent. **c** PEI percent and GA activation time. **d** PEI activation time and GA percent. **e** PEI activation time and GA activation time. **f** GA percent and GA activation time

interaction terms (WX, XY, XZ) and quadratic terms (W^2, Y^2) were insignificant ($P > 0.05$). As shown in Fig. 4 the Pareto chart interpreted that GA (%) possessed the most significant influence flowed by PEI activation time and PEI (%) that affected IY of α-amylase positively, whereas GA activation time exhibited negatively significant effect. The validation of the model was achieved from the closing between the actual and predicted IY values as presented in Fig. 5. The normality assumption was satisfied as the residual plot approximated along a straight line as given in Fig. 6. Demonstrating the fitness and influence of CCD statistical model to optimize beads modification conditions for α-amylase immobilization agrees with the findings of Singh et al. (2015). The 3D response surface plots supply an explanation of the interaction between two factors while preserving the other variables at zero level as observed in Fig. 7a–f. The 3D surface interactions determined the optimum levels of independent variables that gave maximum immobilization yield of α-amylase and also revealed the significance of these interactions. Finally, optimization of beads modifications enhanced the IY by 1.5-fold compared with un-optimized.

Scanning electron microscopy showed the modification that happened before and after enzyme conjugation (immobilization). As shown in Fig. 8 a and b, a remarkable change in pore size can be recognized as the gel

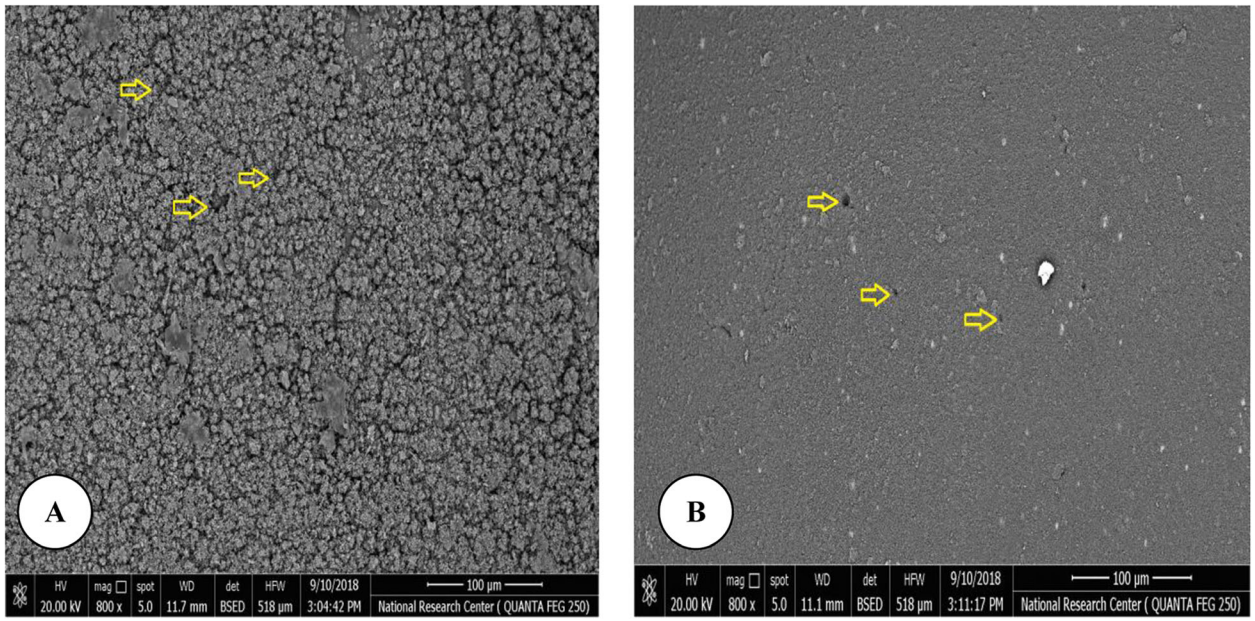

Fig. 8 Scanning electron microscope (SEM) showed the difference in pore size of activated Ch-MNP beads (**a**) and Ch-MNP/PEI/GA/Enz (**b**)

beads exhibited pores before coupling with enzyme molecule. While after immobilization, the enzyme particles were accumulated on the bead surfaces and the pores were decreased in size and tend to disappeared (Ahmed et al. 2018). The changes in morphology of composites in SEM structural analysis indicate their interaction as pointed by Nasir et al. (2017).

FTIR spectroscopic analysis determined the typical characteristic absorption bands of activated beads (Ch-MNP/PEI/GA) (A), immobilized α-amylase on activated beads (Ch-MNP/PEI/GA/Enz) (B), and free α-amylase enzyme (C). As displayed in Fig. 9, activated beads showed two peaks, one of them at 1730 cm^{-1} corresponding to the (C=O) group of GA free end, and the second one is at 1650 cm^{-1} corresponding to the (C=N–) group that was produced from the reaction with GA (curve A). Whereas, Ch-MNP/PEI/GA/Enz gives broader peak at 3457 cm^{-1}, pointed to increasing NH_2 group's concentration (curve B). When comparing with free α-amylase enzyme (curve C) we can notice that, the characteristic peaks of enzyme, at 3434 cm^{-1} and at 1117 cm^{-1}, are found in curve (B). From these data, it was revealed that the processes of

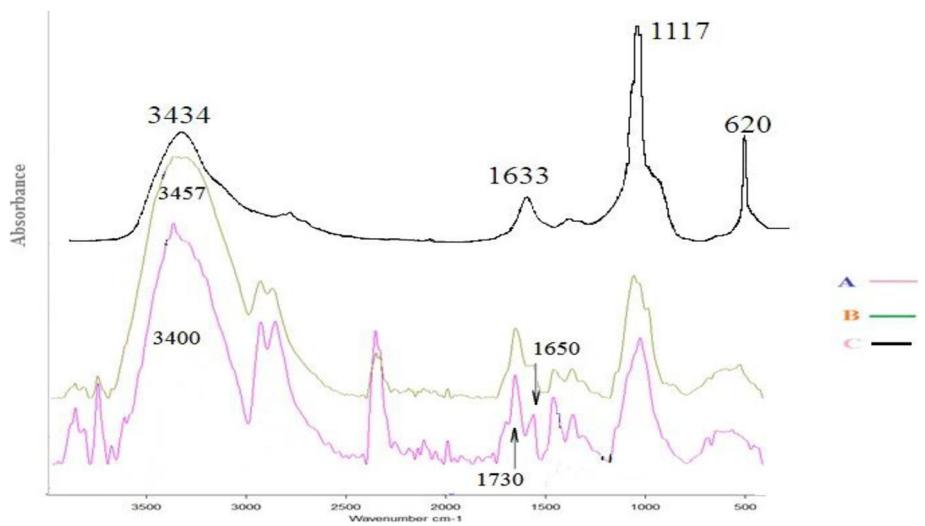

Fig. 9 FT-IR of activated beads (Ch-MNP/PEI/GA) (A), immobilized enzyme (Ch-MNP/PEI/GA/Enz) (B) and free enzyme (C)

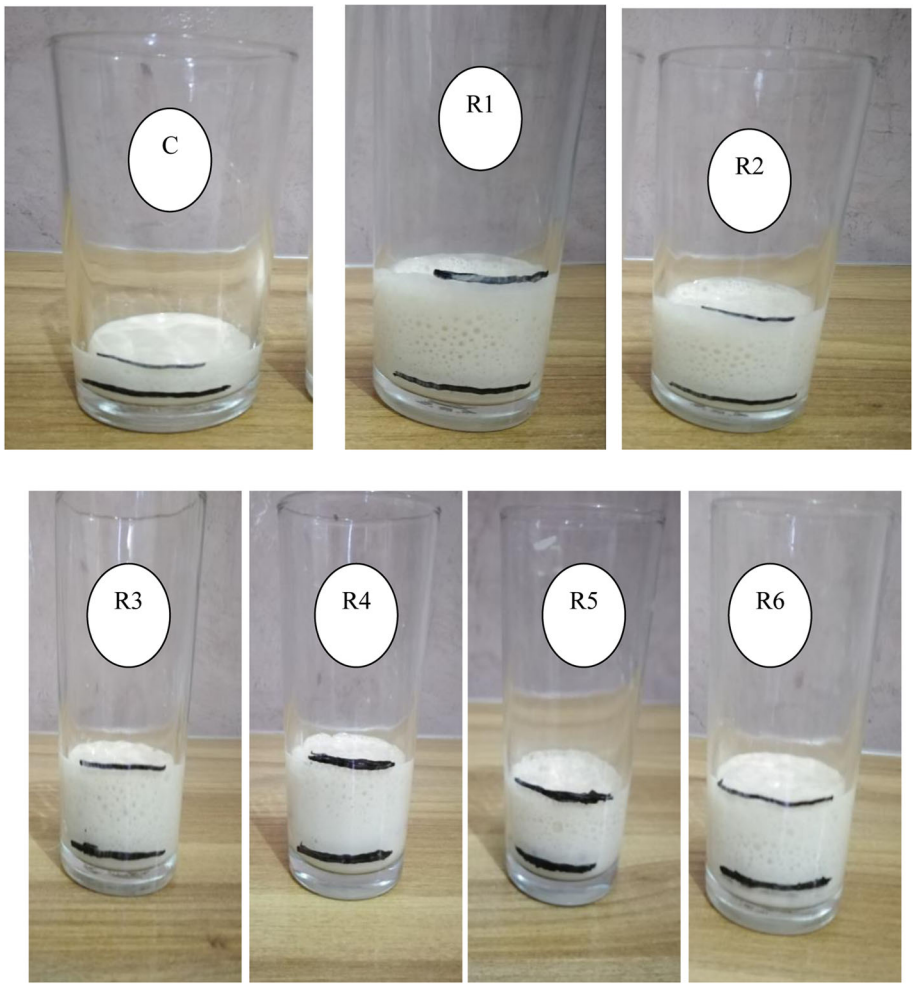

Fig. 10 Application of immobilized α-amylase and its reusability for dough-raising in bakery (R1, R2, R3, R4, R5 and R6) and control without α-amylase addition (C)

amination, activation, and immobilization were successful. These results were in agreement with the results obtained by other published results (Yuan et al. 2016). Díaz-Hernández et al. (2018) reported that the change in intensity as well as the displacement of the NH_2, C–O, and Fe bands after cross-linking suggests the formation of covalent bonds between enzymes and the magnetic beads. From characterization steps, FTIR and SEM, it was concluded that the process of activation and immobilization takes place successfully as pointed by Hassan et al. (2019).

By applying immobilized α-amylase (Ch-MNP/PEI/GA/Enz) in baking process it was found that, Ch-MNP/PEI/GA/Enz enhanced dough-raising about 2.3-fold as compared to the control (without enzyme) as shown in Fig. 10. Also, Ch-MNP/PEI/GA/Enz could be reused for 5 consecutive cycles with 100% residual activity. The results pointed to the possibility of safely using of Ch-MNP/PEI/GA/α-amylase enzyme for application in the baking industry. This result might be due to reducing the staling rate of the crumb and increasing the bread volume by α-amylase (Kaltsa et al. 2013).

Conclusion

α-Amylase was successfully immobilized on chitosan-magnetic nano-particles (Ch-MNP/PEI/GA) with high IY%. SEM and FTIR studies confirm the linkage between Ch-MNP/PEI/GA beads and the α-amylase enzyme. Optimized conditions using statistical methods (CCD) enhanced IY% from 55 to 81.6%. The highest IY of α-amylase was obtained at 6% PEI for 4 h activation time and 4% GA for 2 h activation time. The ANOVA data confirmed the great significance of the model which possessed F value of 27.914. Also, the adjusted R^2 value was 0.940 and closer to R-square value which demonstrated the suitability of this model which improved IY% by 1.5-fold compared to un-optimized process. The Ch-MNP/PEI/GA/Enz is suitable for application in baking industry and enhanced dough-raising about 2.3-fold as compared to the control.

Abbreviations

RSM: Response surface methodology; ANOVA: Analysis of variance; CCD: Central composite design; Ch-MNP: Chitosan-magnetic nano-particles; Ch-MNP/PEI/GA/Enz: Chitosan-magnetic nano-particles/polyethyleneimine/glutaraldehyde/Enzyme; Df: Degree of freedom; DNS: Dinitrosalicylic acid; FTIR: Fourier transforms infrared; SEM: Scanning electron microscope; GA: Glutaraldehyde; IY: Immobilization yield; PEI: Polyethylenimine; R^2: Coefficient of determination; RSM: Response surface methodology; DD: Degree of deacetylation; Mw: Molecular weight

Acknowledgements

The authors are very thankful to the National Research Centre for providing financial assistance to carry out this research.

Authors' contributions

This research was extracted from PhD thesis. Mohamed A.A. Abdella performed the practical experiments, the statistical design, and contributed to the writing of the manuscript with Samia A. Ahmed. All authors participated in every step of this work, read and approved the final manuscript.

Authors' information

Mohamed A.A. Abdella, Aliaa R. El-Shamy, Sherien M.M. Atalla, and Samia A. Ahmed are from the Chemistry of Natural and Microbial Products Department, National Research Centre, Dokki, Cairo, Egypt.
Gamal M. El-Sherbiny is from the Department of Botany and Microbiology, Faculty of Science (Boys), Al-Azhar University, Cairo, Egypt.

Funding

This research was a part of PhD thesis that was funded by the National Research Centre.

Availability of data and materials

All data generated or analyzed during this study are included in this manuscript.

Ethics approval and consent to participate

Not applicable.

Consent for publication

All authors have read and approved to submit it to the Bulletin of the National Research Centre. There is no conflict of interest of any author in relation to the submission.

Competing interests

The authors declare that they have no competing interests.

Author details

[1]Chemistry of Natural and Microbial Products Department, National Research Centre, Dokki, Cairo, Egypt. [2]Department of Botany and Microbiology, Faculty of Science (Boys), Al-Azhar University, Cairo, Egypt.

Received: 16 December 2019 Accepted: 12 March 2020
Published online: 20 March 2020

References

Abdel Wahab WA, Ahmed SA (2018) Response surface methodology for production, characterization and application of solvent, salt and alkali-tolerant alkaline protease from isolated fungal strain *Aspergillus niger* WA 2017. Int J Biol Macromol 115:447–458

Abdel Wahab WA, Karam EA, Hassan ME, Kansoh AL, Esawya MA, Awad GE (2018) Optimization of pectinase immobilization on grafted alginate-agar gel beads by 24 full factorial CCD and thermodynamic profiling for evaluating of operational covalent immobilization. Int J Biol Macromol 113:159–170

Ahmed SA, Abdella MAA, El-Sherbiny GM, Ibrahim AM, El-Shamy AR, Atalla SMM (2019b) Application of one –factor- at-a-time and statistical designs to enhance α-amylase production by a newly isolate Bacillus subtilis strain-MK1. Biocat Agricul Biotech 22:101397

Ahmed SA, Al-domany RA, El-Shayeb NM, Radwan HH, Saleh SA (2008) Optimization, immobilization of extracellular alkaline protease and characterization of its enzymatic properties. Res J Agric Biol Sci 4:434–446

Ahmed SA, Mostafa FA, Ouis MA (2018) Enhancement stability and catalytic activity of immobilized α-amylase using bioactive phospho-silicate glass as a novel inorganic support. Int J Biol Macromol 112:371–382

Ahmed SA, Saleh SAA, Abdel-Hameed SAM, Fayad AM (2019a) Catalytic, kinetic and thermodynamic properties of free and immobilized caseinase on mica glass-ceramics. Heliy 5:e01674 https://doi.org/10.1016/j.heliyon.2019.e01674

Ahmed SA, Saleh SAA, Mostafa FA, Abd El Aty AA, Ammar HAM (2016) Characterization and valuable applications of xylanase from endophytic fungus *Aspergillus terreus* KP900973 isolated from *Corchorus olitorius*. Biocat Agricul Biotech 7:134–144

Atacan K, Çakıroglu B, Özacar M (2016) Improvement of the stability and activity of immobilized trypsin on modified Fe3O4 magnetic nanoparticles for hydrolysis of bovine serum albumin and its application in the bovine milk. Food Chem 212:460–468

Bindu VU, Shanty AA, Mohanan PV (2018) Parameters affecting the improvement of properties and stabilities of immobilized α-amylase on chitosan-metal oxide composites. Inter J Biochem Biophys 6:44–57

Díaz-Hernández A, Gracida J, García-Almendárez BE, Regalado C, Núñez R, Amaro-Reyes A (2018) Characterization of magnetic nanoparticles coated with chitosan: a potential approach for enzyme immobilization. Hind J of Nanom 2018:9468574

Eskandarloo H, Abbaspourrad A (2018) Production of galacto-oligosaccharides from whey permeate using β-galactosidase immobilized on functionalized glass beads. Food Chem 251:115–124

Frantz SC, Paludo LC, Stutz H, Spier MR (2019) Production of amylases from Coprinus comatus under submerged culture using wheat-milling by-products: optimization, kinetic parameters, partial purification and characterization. Biocat Agricul Biotech 17:82–92

Hassan ME, Yang Q, Xiao Z (2019) Covalent immobilization of glucoamylase enzyme onto chemically activated surface of κ-carrageenan. Bull of the Nat Res Cent 43:102–112

Jaya E., Aslania P, Raynor DK (2010) User testing of consumer medicine information in Australia. Heal Educa J 70: 420-427.

Kaltsa O, Georgopoulos T, Yanniotis S, Mandala L (2013) Effect of enzyme blends and dough strengthening emulsifier on extending the shelf life of sandwich bread applying response surface methodology. Inter J Innov Resear Sci Eng Technol 3(4):149–160

Kuo C-H, Liu Y-C, Chang C-MJ, Chen J-H, Chang C, Shieh C-J (2012) Optimum conditions for lipase immobilization on chitosan-coated Fe3O4 nanoparticles. Carbohydr Polym 87:2538–2545

Mehta RV, Desai R, Bhat P, Upadhyay RV (2006) Synthesis and characterization of certain nanomagnetic particles coated with citrate and dextran molecules. Ind J pure appl phys 44:537–542

Miller GL (1959) Use of dinitrosalicylic acid reagent for determination of reducing sugar. Anal Chem 31:426–428

Misson M, Zhang H, Jin B (2015) Nanobiocatalyst advancements and bioprocessing applications. J Roy Soci Interf 12:1–20

Nasir Z, Shakir M, Wahab R, Shoeb M, Alam P, Khan RH, Mobin M, Lutfullah (2017) Co-precipitation synthesis and characterization of Co doped SnO_2 NPs, HSA interaction via various spectroscopic techniques and their antimicrobial and photocatalytic activities. Int J Biol Macromol 94:554–565

Pandey G, Munguambe D, Tharmavaram M, Rawtani D, Agrawal Y (2017) Halloysite nanotube - an efficient 'nano-support' for the immobilization of α-amylase. Appl Clay Sci 136:184–191

Sajjad M, Choudhry S (2012) Effect of starch containing organic substrates on alpha amylase production in *Bacillus strains*. Afr J Microbiol Res 6:7285–7291

Simair AA, Qureshi AS, Khushk I, Ali CH, Lashari S, Bhutto MA, Mangrio GS, Lu C (2017) Production and partial characterization of α-amylase enzyme from *Bacillus sp.* BCC 01-50 and potential applications. BioMed Resea Inter 2017:1–9

Singh K, Srivastava G, Talat M, Srivastava ON, Kayastha AM (2015) α Amylase immobilization onto functionalized grapheme nanosheetsas scaffolds: its characterization, kinetics and potential applications in starch based industries. Biochem Biophys Rep 3:18–25

Sojitra UV, Nadar SS, Rathod VK (2017) Immobilization of pectinase onto chitosan magnetic nanoparticles by macromolecular cross-linker. Carbohydr Polym 157:677–685

Souza CJ, Garcia-Rojas EE, Souza CS, Vriesmann LC, Vicente J, de Carvalho MG, Petkowicz CL, Favaro-Trindade CS (2019) Immobilization of β-galactosidase by complexation: effect of interaction on the properties of the enzyme. Int J Biol Macromol 122:594–602

Swelam AA, Awad MB, Gedamy YR, Tawfik A (2019) Fe3O4 Nanoparticles: synthesis, characterization and application in removal of iron from aqueous solution and groundwater. Egypt J Chem 62:1189–1209

Tambekar DH, Tambekar SD, Rajgire AV, Jadhav AS, Sawale KK (2016) Isolation and characterization of amylase from *Lysinibacillus Xylanilyticus* from alkaline environment. Inter J Res Stud Biosci 4:1–4

Wang X-Y, Jiang X-P, Li Y, Zeng S, Zhang Y-W (2015) Preparation Fe3O4@chitosan magnetic particles for covalent immobilization of lipase from *Thermomyces lanuginosus*. Int J Biol Macromol 75:44–50

Yang X, Lee JH, Yoo HY, Shin HY, Thapa LP, Park C, Kim SW (2014) Production of bioethanol and biodiesel using instant noodle waste. Biopro Biosys Engin 37(8):1627–1635

Yuan Y, Luan X, Rana X, Hassan ME, Dou D (2016) Covalent immobilization of cellulase in application of biotransformation of ginsenoside Rb1. J Molecu Cata B: Enzy 133:S525–S532

Zdarta J, Meyer AS, Jesionowski T, Pinelo M (2018) A general overview of support materials for enzyme immobilization: characteristics, properties, practical utility. Cataly 8:1–27

Publisher's Note